Spectrochimica Acta Part A: Molecular and Biomolecular Spectroscopy 112 (2013) 343–350

Contents lists available at SciVerse ScienceDirect

Spectrochimica Acta Part A: Molecular and Biomolecular Spectroscopy

journal homepage: www.elsevier.com/locate/saa

FT-IR, FT-Raman spectra and DFT calculations of melaminium perchlorate monohydrate

N. Kanagathara [a], M.K. Marchewka [b], M. Drozd [b], N.G. Renganathan [c], S. Gunasekaran [d], G. Anbalagan [e,*]

[a] Department of Physics, Vel Tech Multi Tech Dr. Rangarajan Dr. Sakunthala Engg. College, Avadi, Chennai 600 062, India
[b] Institute of Low Temperature and Structure Research, Polish Academy of Sciences, 50-950 Wrocław, 2, P.O. Box 937, Poland
[c] Department of Chemistry, Vel Tech Dr. RR Dr. SR Technical University, Avadi, Chennai 600 062, India
[d] PG and Research Department of Physics, Pachaiyappa's College, Chennai, India
[e] Department of Physics, Presidency College, Chennai 600 005, India

HIGHLIGHTS

- Melaminium perchlorate mono hydrate single crystals have been synthesized.
- The crystal system was identified as triclinic ($P-1$) and characterized by FT-IR, FT-Raman, FT-NMR studies.
- Several stretching and deformation modes confirm the presence of extensive intermolecular hydrogen bonding in the crystal.
- The optimized geometry and vibrational frequencies are calculated using DFT.
- HOMO–LUMO energies are calculated and show that charge transfer occurs within the molecule.

GRAPHICAL ABSTRACT

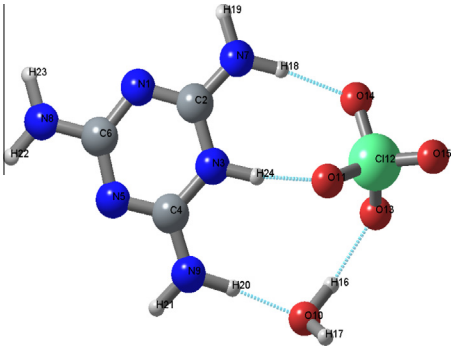

ARTICLE INFO

Article history:
Received 25 September 2012
Received in revised form 23 March 2013
Accepted 1 April 2013
Available online 23 April 2013

Keywords:
Crystal growth
Fourier transforms infrared
Fourier transform Raman
DFT calculations
Hydrogen bonds

ABSTRACT

Melaminium perchlorate monohydrate (MPM), an organic material has been synthesized by slow solvent evaporation method at room temperature. Powder X-ray diffraction analysis confirms that MPM crystal belongs to triclinic system with space group $P-1$. FTIR and FT Raman spectra are recorded at room temperature. Functional group assignment has been made for the melaminium cations and perchlorate anions. Vibrational spectra have also been discussed on the basis of quantum chemical density functional theory (DFT) calculations using Firefly (PC GAMESS) version 7.1 G. Vibrational frequencies are calculated and scaled values are compared with experimental values. The assignment of the bands has been made on the basis of the calculated PED. The Mulliken charges, HOMO–LUMO orbital energies are analyzed directly from Firefly program log files and graphically illustrated. HOMO–LUMO energy gap and other related molecular properties are also calculated. The theoretically constructed FT-IR and FT-Raman spectra of MPM coincide with the experimental one. The chemical structure of the compound has been established by ^{1}H and ^{13}C NMR spectra. No detectable signal was observed during powder test for second harmonic generation.

1. Introduction

Melamine (2,4,6-triamino-1,3,5-triazine) has wide applications in industry as a fire retardant substance. The use of melamine resin in automobile paints was examined by Zieba-Palus [1]. A lot of theoretical works were performed to explain the behavior of melamine molecule in the solid state [2–7]. Melamine complexes form the class of compounds that crystallize with interesting hydrogen-bond networks. The crystal structure of melaminium perchlorate monohydrate was published by Zhao et al. [8]. According to the data presented there, MPM consists of melaminium cat-

* Corresponding author. Tel.: +91 9487140051.
E-mail address: anbu24663@yahoo.co.in (G. Anbalagan).

1386-1425/$ - see front matter © 2013 Elsevier B.V. All rights reserved.
http://dx.doi.org/10.1016/j.saa.2013.04.001

ions $C_3H_7N)_6^+$, perchlorate anions ClO_4^- and water molecules. Generally, the solid state complexation of melamine with different organic and inorganic (mineral) acids has an interesting aspect concerning the hydrogen bond system formed. Such a system comprises most frequently the N–H···O and O–H···O types [4]. Generally, Spectroscopic methods are expected to provide a detailed knowledge of any molecular framework. Also they provide information on the type of symmetry present in the molecule, the nature of chemical bonds involved, the behavior of normal modes and the effect of various types of intermolecular forces. Many vibrational studies have been reported for hydrogen bonded system. A number of spectroscopic studies of melamine with inorganic acids have already been reported by Marchewka et al. [9–14]. Perchloric acid forms interesting complexes with organic cations. Perchlorates are interesting due to structural phase transition connected with the ordering of perchlorate anions [15–18]. Several researchers studied the perchlorate anion with amino acids [19–22]. In this work, we report the growth of melaminium perchlorate monohydrate (MPM). The grown crystal was characterized by X-ray diffraction. Density Functional Theory (DFT) calculations are performed in order to analyze studied molecules. The optimized structures of MPM complex have been calculated by the DFT/B3LYP method. The 6-311++G(d,p) basis set have been employed. To establish the chemical structure of MPM, NMR studies have also been carried out. The results are presented and discussed in detail.

2. Experimental

2.1. Synthesis and crystal growth

Melaminium perchlorate monohydrate ($C_3H_7N_6^+ClO_4^- \cdot H_2O$) crystals were grown by slow solvent evaporation technique. The double distilled water was used as a solvent. AR grade samples of melamine and perchloric acid were taken in 1:2 ratio. The dissolved acid was added drop wise to the hot solution of melamine. The solution was stirred well using magnetic stirrer, filtered and then allowed to cool at room temperature. Tiny, transparent, colorless crystals were grown after 3–4 weeks duration.

2.2. Characterization

The grown crystals have been subjected to various characterization studies like X-ray powder diffraction, FT-IR and FT-Raman, FT-NMR and SHG. The grown crystals have been characterized by X-ray powder diffraction technique using Rich Seifert X-ray powder diffractometer with CuK_α radiation of $\lambda = 1.5406$ Å in the 2θ range 10–70° by employing the reflection mode for scanning. The detector used was a scintillation counter. The sample was scanned at a rate of 1° min^{-1}. A Perkin Elmer Spectrum one FT-IR spectrometer was employed to record the IR spectrum to analyze the functional groups present in the crystals. The sample for this measurement was finely grounded and mixed with KBr. Raman spectral measurements were made with a FT-Raman Bruker RFS 100/S Raman module. An air cooled diode pumped Nd:YAG laser, operated at 1064 nm and a power output of 150 mW was used as source. The spectrum was recorded over the range 3500–50 cm^{-1}. Proton NMR and carbon NMR spectra were recorded using D_2O as solvent on a Bruker Avance III 500 MHz spectrometer at 22 °C to confirm the molecular structure of the grown crystal. The grown crystals of melaminium perchlorate monohydrate was subjected to Kurtz second harmonic generation test by using Nd:YAG Q switched laser beam with input pulse of 5.2 mJ for the non-linear optical property.

2.3. Computational details

All calculation were performed with the Firefly (PC GAMESS) version 7.1.G, build number 5618 program [23] compiled under Linux operating system. This job was executed on small PC Cluster consisting of three server nodes with 32-bit and 64-bit AMD processors running at 1.8 GHz and 2 GB RAM. The MPICH [24] implementation of MPI standard (Message Passing Interface) for communication between cluster nodes was used. This protocol ensures good performance and complete remote execution environment. For calculation the structural data from X-ray investigation of MPM crystal was used [8]. The coordinates for particular atoms were established and the Z-matrix was built by Molden program [25]. The Z-matrix was directly used in input Firefly files. The optimized structures for all investigated forms of considered complex have been calculated by the DFT/B3LYP method. The 6-311++G(d,p) basis set have been employed. The harmonic frequencies, infrared intensities and Raman activities were calculated by the density functional triply parameter hybrid model (DFT/B3LYP) with identical basis set. According to theoretical calculations, the structure with energy of form which was geometrically nearest to X-ray data, one negative frequency was obtained (see Table 4). It is clear that global minimum was not calculated [26]. Similar situation was observed in Ethylenediammonium complex [27]. The normal coordinate analysis has been carried out for investigated molecule according to the procedure described and recommended by Fogarasi and Pulay [28]. The frequencies due to stretching vibrations were scaled by 0.96. The calculated potential energy distribution (PED) for the investigated molecule has enabled us to make detailed band assignment in infrared and Raman spectra. The Mulliken charges, HOMO and LUMO orbitals energies were analyzed directly from Firefly program log files. The graphic interpretation of mentioned properties was made by Modeling and Simulation Kit (MASK) program (version 1.3.0) [29]. In the cases of HOMO, LUMO and electrostatic potentials graphic illustrations of the isosurface with value equal to 0.01 was used.

3. Results and discussion

3.1. Powder XRD analysis

The crystallinity was confirmed through powder X-ray diffraction analysis and from the indexed X-ray powder diffraction pattern, the unit cell parameters were calculated as $a = 5.5625 \pm 0.0765$ Å, $b = 7.7785 \pm 0.0935$ Å, $c = 11.9622 \pm 0.1560$ Å, $\alpha = 102.97 \pm 0.60°$, $\beta = 96.35 \pm 0.82°$, $\gamma = 109.26 \pm 0.69°$ and $V = 466.45$ Å^3. The calculated values agree very well with earlier literature [8].

3.2. Vibrational analysis

3.2.1. FTIR studies

The FTIR spectrum of MPM crystal is shown in Fig. 1 and the vinrational assignments are presented in Table 1. The internal vibrations of melamine molecule were already published [2–6]. According to crystallographic data, melaminium residues often form hydrogen bonds of N–H···N and N–H···O type. The bands observed in the measured region 4000–400 cm^{-1} arise from internal vibrations of melaminium cations, perchlorate anions and water molecules. The bands below 200 cm^{-1} in the Raman spectra arise from the lattice vibrations of the crystal [12]. The NH_2 theoretical stretching frequencies of neutral molecule of melamine have been determined by Fernandez-Liencres et al. [30]. NH_2 symmetric stretching of vibration occurs at 3345 cm^{-1} and generally this peak

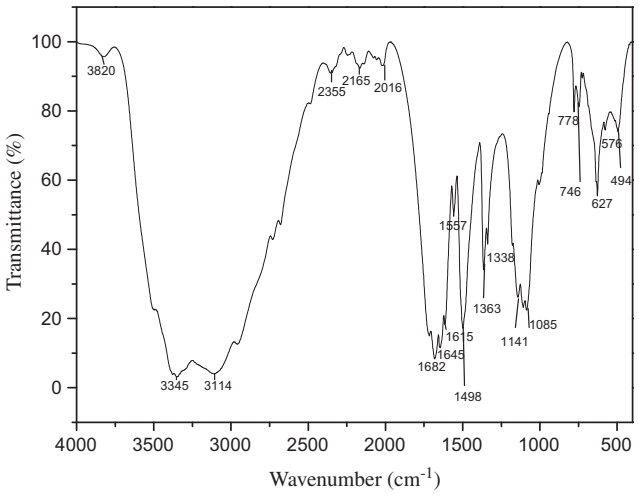

Fig. 1. FT-IR spectrum of MPM.

appears at 3328 cm^{-1} for melamine crystal. The difference of 17 cm^{-1} corresponds to well known blue shift. The calculated PED has revealed that the NH_2 symmetric vibration of melaminium cations occurs at 3357 cm^{-1}.

The peak at 2355 cm^{-1} was attributed to the vibrations of hydrogen bond formed by water molecules [12–14,18,24]. Several pronounced differences have been noticed between the infrared spectrum of melamine crystal and that for melaminium perchlorate monohydrate in the region of NH_2 bending type of vibration. The weak bands at 1682 cm^{-1} and 1557 cm^{-1} which may be due to intermolecular interaction through the NH_2 groups of melamine molecule that causes the rising of their frequencies for bending type of motions [32] and these peaks usually occur at 1650 cm^{-1} and 1551 cm^{-1} [3]. The weak band at 1498 cm^{-1} was assigned to N–H deformation vibration [28]. The peak with moderate intensity appears at 1363 cm^{-1} was assigned to the semi-circle stretching vibrations mechanically coupled with exogenous C–N contract and NH bending vibration [4]. The medium peaks at 1338 cm^{-1} and 1141 cm^{-1}were assigned to semi circle stretching vibration [7] and NH_2 rocking vibration [3] respectively. The band at 814 cm^{-1} in infrared spectrum of melamine crystal, originates from bending type of vibration of triazine ring was moved to the lower wave number at 778 cm^{-1} in the present case [12] may be due to the perchlorate anion. The peak with medium intensity appears at 1085 cm^{-1} was due to the ClO_4^- asymmetric stretching vibration [33]. The strong IR band at 746 cm^{-1} was assigned to ring bending vibration [3,32,34]. The peak at 627 cm^{-1} [35] was assigned to ClO_4^- asymmetric bending type of vibration. The IR band at 576 cm^{-1} was attributed to side chain in plane C–N bending vibration [3].

3.2.2. FT Raman studies

The FT Raman of MPM is shown in Fig. 2 and the vibrational assignments are given in Table 1. Raman band at 1442 cm^{-1} in melamine crystals originates from NH_2 bending type of vibration was moved to higher wave numbers i.e. 1554 cm^{-1} and 1505 cm^{-1} in the present case [32]. The peak at 1606 cm^{-1} was assigned to in-plane deformation type of vibration. Weak Raman band at 981 cm^{-1} originates from triazine ring N in-phase radial type of vibration instead of 984 cm^{-1} [7,34]. Such bands are present in FT-Raman spectrum of many melamine complexes. The most intense or strong band at 687 cm^{-1} was due to symmetric vibrations of triazine ring. This is an excellent Raman group frequency and it is found in Raman spectra of all melamine complexes [31]. This band usually occurs at 676 cm^{-1} for melamine crystal

Table 1
Vibration band assignment of MPM.

Wave number cm^{-1}		Assignment	Refs.
FT-IR	FT-Raman		
3345		NH_2 symmetric stretching of vibration	[25]
3114		N–H···N stretching	
2355		Vibrations of hydrogen bonds formed by water molecules	[12–14,18,31]
1682		NH_2 bending	[3]
1645		H_2O in-plane bend	[12]
1615		H_2O in-plane bend	[12]
1557	1554	NH_2 bending vibration	[3,32]
1498	1505	N–H deformation vibration	[30]
1363		Semi-circle stretching vibrations mechanically coupled with exogenous C–N contract, CH_3 in phase bend and the NH bending vibration	[4]
1338	1339	Semi-circle stretching vibrations mechanically coupled with exogeneous C–N contract, CH_3 in phase bend and the NH bending vibration	[4,7]
1141		NH_2 rocking vibration	[3]
1085	1077	ClO_4^- asymmetric stretching vibration	[33,39]
	981	Triazine ring N in phase radial type of vibration	[7,31]
	937	ClO_4^- symmetric stretching	[33]
778		Ring sextant out of plane bending	[3]
746		Ring bend, ring bend out of plane	[3,32,34]
	687	Symmetric vibrations of triazine ring	[31]
627	630	ClO_4^- asymmetric bending type of vibration	[35]
576	570	C–N bending vibration	[3]
494		Combination tone: NH_2 bend –NH_2 rock	[3]
	462	ClO_4 torsion mode of vibration	[35]
	365	NH_2 torsion	[18]
	215	Lattice vibration	[33]
	104	Lattice vibration	[33]

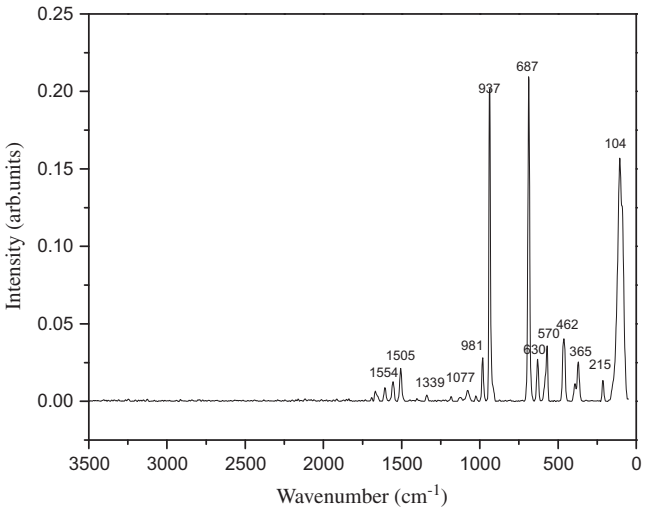

Fig. 2. FT-Raman spectrum of MPM.

[12]. The complexation of melamine causes, in all cases, the rising of the frequency of this vibration compared to the value of melamine alone. It is suggested, that due to number of intense ionic and donor–acceptor types of interaction with environment, the s-triazine ring becomes more rigid [32]. The band at 570 cm^{-1} was assigned to the ring bending type of vibration. In the case of melamine crystal, the corresponding Raman band was observed at 582 cm^{-1} [3]. Several investigators have studied IR and Raman spectra of perchlorate ion [36–38]. The ClO_4^- ion adopts a regular tetrahedral structure and has nine different vibration degrees of freedom and has co-ordination through hydrogen bonding [21]. The four normal modes of vibration of free ClO_4^- are expected to occur at 930 cm^{-1}, 459 cm^{-1}, 1102 cm^{-1} and 625 cm^{-1} [36,37]. The weak band at 1339 cm^{-1} was assigned to the semi-circle stretching vibrations mechanically coupled with exogeneous C–N contract and the NH bending vibration [4]. The intense sharp peak at 937 cm^{-1} and medium peak at 630 cm^{-1} were assigned to ClO_4^- symmetric stretching and ClO_4^- anti symmetric bending vibration respectively [35]. This indicates that the perchlorate anion with tetrahedral symmetry is not affected. The very weak band at 1077 cm^{-1} was assigned to ClO_4^- anti symmetric stretching [39] and peak at 462 cm^{-1} with weak intensity was assigned to ClO_4 torsion mode of vibration [35].

3.2.3. Computational results

The DFT has long been recognized as a better alternative tool in the study of organic, inorganic chemical systems. In the present study, DFT technique was employed to study the complete vibrational spectrum of MPM and to identity the various normal modes with greater wave number of accuracy. Fig. 3 shows the optimized geometric molecular structure of MPM. The optimized geometrical parameters obtained by the DFT calculation were presented in Table 2 in accordance with the atoms numbering given in Fig. 3. It was found that bond length, bond angles of MPM predicted by the DFT calculations are very close to the reported values [8]. The calculated C–N distances are similar to the values reported by Zhao et al. [8] except two distances C(6)–N(8) and C(6)–N(5). The theoretical calculations give the C–N distances in the range 1.34–1.35 Å. The calculated N–H distances are very similar to those obtained by Zhao et al. [8]. But there is a lit bit difference in N(3)–H(24), N(7)–H(18) and N(9)–H(20) because of hydrogen involvement in intermolecular N–H···O interactions (~1.043 Å). There exists a small difference between theoretical and experimental values for Cl–O distances, but the differences are very small. On the basis of performed DFT calculation, it is clear that Cl(12)–O(14) and Cl(12)–O(13) are identical i.e. 1.506 Å but Cl(12)–O(11) and Cl(12)–O(15) are not identical and their distances are 1.529 Å and 1.473 Å respectively. During calculation, two intermolecular hydrogen bonds N(9)–H(20)···O(10), N(3)–H(24)···O(11) are observed and their bond lengths are equal to 2.807 Å and 2.744 Å respectively. All fundamental modes of vibrations are active both in FT-IR and FT-Raman. The theoretically calculated frequencies seem to be in good agreement with experimental values. The obtained DFT calculation results are tabulated in Table 3. Fig. 4 shows the theoretically constructed FT-IR and FT-Raman spectrum which agrees well with the experimental one.

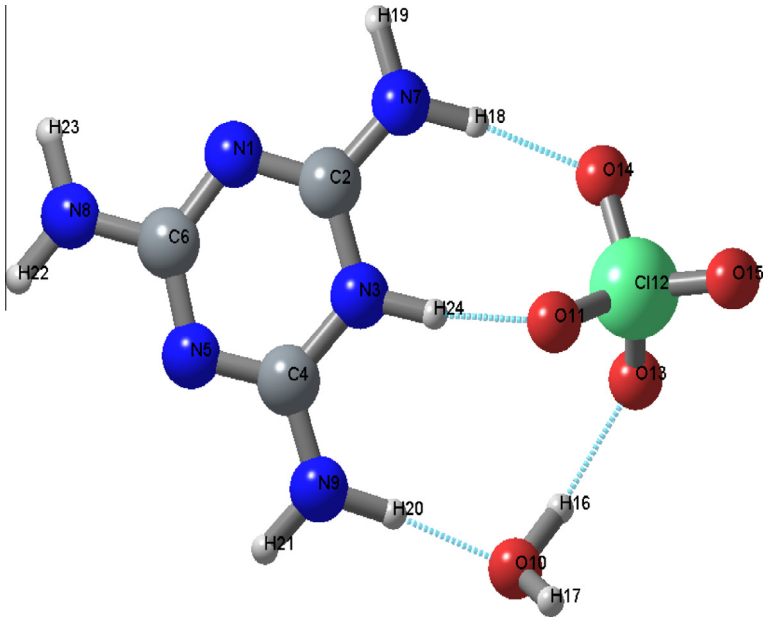

Fig. 3. Optimized structure of MPM.

Table 2
Optimized Geometry parameters.

Bond	Length (Å)	Bond angle	(°)	Dihedral angle	(°)
C2–N3	1.374	C2–N3–C4	118.956	C2–N3–C4–N5	−3.602
C2–N7	1.333	C2–N3–H24	119.179	C2–N3–C4–N9	176.777
C4–N5	1.330	C2–N3–O11	113.650	C2–N3–O11–CL12	−71.890
C4–N9	1.332	C2–N7–H18	121.871	C4–N3–C2–N7	−176.828
C6–N8	1.345	C2–N7–H19	116.861	C4–N5–C6–N8	−177.822
CL12–O13	1.506	C4–N5–C6	115.749	C4–N9–O10–H16	−10.492
CL12–O14	1.507	C4–N9–H20	123.847	C4–N9–O10–H17	111.731
CL12–O15	1.473	C4–N9–H21	116.048	N1–C2–N3–C4	3.699
N1–C2	1.328	C4–N9–O10	126.616	N3–C2–N7–H18	13.168
N3–C4	1.373	C6–N8–H22	119.583	N3–C2–N7–H19	177.757
N3–H24	1.043	C6–N8–H23	119.581	N3–C4–N5–C6	0.421
N3–O11	2.744	N1–C2–N3	121.585	N3–C4–N9–H20	−11.255
N5–C6	1.348	N3–C2–N7	117.771	N3–C4–N9–H21	−177.739
N7–H18	1.024	N3–C4–N5	121.294	N3–C4–N9–O10	−15.654
N7–H19	1.009	N3–C4–N9	118.223	N3–O11–CL12–O13	−72.520
N8–H22	1.008	N3–O11–CL12	115.142	N3–O11–CL12–O14	44.963
N8–H23	1.008	N5–C6–N8	116.676	N3–O11–CL12–O15	166.143
N9–H20	1.034	N9–O10–H16	112.619	N5–C6–N8–H22	−1.236
N9–H21	1.010	N9–O10–H17	117.801	N5–C6–N8–H23	−178.007
N9–O10	2.807	O11–CL12–O13	107.618	N7–C2–N3–H24	10.245
O10–H16	0.980	O11–CL12–O14	107.205	N7–C2–N3–O11	15.554
O10–H17	0.966	O11–CL12–O15	110.020		
O11–CL12	1.529				

Table 3
Calculated wavenumbers (in cm^{-1}) of FT-IR and FT-Raman spectra of MPM by DFT/B3LYP method.

Frequency (cm^{-1})	Scaled frequency (cm^{-1})	Intensity (km/mol)	Raman activity (AU)	PED % (more than 10%)	Assignment
3882	3727	85	54.6	O10–H17 98	ν_{as}OH
3765	3614	81	53.3	N8–H23 60, N8–H22 40	ν_{as}NH
3696	3549	135	70.3	N7–H19 96	ν_{as}NH
3660	3513	83	83.4	N9–H21 98	ν_{as}NH
3619	3474	130	166.0	N8–H22 60, N8–H23 40	ν_{as}NH
3586	3442	532	91.9	O10–H16 97	ν_{s}OH
3357	3223	1143	249.4	N7–H18 94	ν_{s}NH
3176	3049	1539	231.9	N9–H20 93	ν_{s}NH
3035	2913	1072	140.6	N3–H24 95	ν_{s}NH
1729	1660	192	8.2	C4–N9–H20 17, C4–N9 15, C2–N7 13, C4–N9–H21 13	δNH, νCN
1712	1643	929	4.0	C2–N3–H24 23, C2–N7 17, C4–N9 11	δNH, νCN
1681	1614	64	0.6	C4–N9–H20 20, C2–N3–H24 15	δNH, δOH
1665	1598	799	1.6	C2–N7–H18 25, N1–C2 22	δNH, νCN
1659	1592	547	4.5	C4–N9–O10–H16 17, C4–N9–O10–H17 14, N9–O10–H16 12	δOH, δNH
1650	1584	58	2.7	C6–N8–H23 17, C6–N8–H22 17, C6–N8 14, C2–N7–H18 13, C4–N9–H20 11	δNH, νCN
1558	1496	7	7.4	C4–N9 15, C4–N5–C6 14, C6–N8–H23 12, C2–N7 11, C6–N8–H22 11, N3–C4 11	νCN, δCN, δNH
1555	1493	314	7.6	N5–C6 41, N3–C4 17, C4–N5–C6 15	νCN, δCN
1485	1426	217	5.3	C6–N8 26, N3–C4–N5 14, C6–N8–H22 10, C6–N8–H23 10	νCN, δNH, δCN
1426	1369	124	4.7	C2–N3–H24 43, C2–N7 17, C4–N9 12	δNH, νCN
1376	1321	6	0.6	C4–N5 24, N1–C2 23, N5–C6 18, C2–N3 15	νCN
1217	1169	12	0.4	C6–N8 18, C2–N3–C4 16	νCN, δCN
1185	1138	4	3.9	C6–N8–H23 14, C6–N8–H22 14, N5–C6–N8 11, C4–N5 10, N1–C2 10	NH, νCN
1131	1086	6	2.7	N3–C4 23, C2–N3 20, C4–N9–H21 14, C2–N7–H19 12	νCN, NH
1090	1047	394	12.9	CL12–O15 77	νClO
1033	992	10	0.8	C2–N3–C4 41, C2–N7–H19 16, C4–N9–H21 12	δCN, NH
1009	968	15	0.8	C6–N8–H2322, C6–N8–H22 22, C4–N5–C6 16, N5–C6 11	NH, δCN
992	952	27	10.2	N3–C4–N5 52, N1–C2–N3 48	δCN
984	944	270	3.7	CL12–O13 46, CL12–O14 42	νClO
956	917	347	2.5	O11–CL12 30, N7–C2–N3–H24 29, CL12–O14 12	νClO, ρNH
889	854	52	4.1	N7–C2–N3–H24 39, O11–CL12 12, N3–C4–N9–H20 11, CL12–O13 11	ρNH, δClO
864	829	53	3.2	N3–C4–N9–H20 68, N7–C2–N3–H24 19	ρNH,
816	783	62	56.0	O11–CL12 41, CL12–O14 21, CL12–O13 20, CL12–O15 13	δClO
792	760	39	0.8	N3–C4–N5–C6 55, N1–C2–N3–C4 40	ρCN
733	704	7	0.7	C2–N3–C4–N5 64, C4–N5–C6–N8 17	ρCN
718	689	4	0.8	C2–N3–C4–N5 45, C2–N3–C4–N9 34, C4–N3–C2–N7 22	ρCN
704	676	155	1.0	N9–O10–H16 55, C4–N9–O10–H16 29	δNHO
690	663	12	27.4	C4–N5–C6 30, C2–N3–C4 19, N3–C4 12, C6–N8 11, N3–C2–N7–H18 10, C4–N5 10	ρCN

(*continued on next page*)

Table 3 (*continued*)

Frequency (cm^{-1})	Scaled frequency (cm^{-1})	Intensity (km/mol)	Raman activity (AU)	PED % (more than 10%)	Assignment
675	648	27	15.0	N3–C2–N7–H18 76, C2–N3–C4–N5 10	NH
586	562	0	6.6	N5–C6–N8–H23 51, N5–C6–N8–H22 44	NH
575	552	20	5.0	C2–N3–C4 41, C4–N5–C6 25	ρCN
570	547	9	4.0	N3–C4–N5 75, N1–C2–N3 20	ρCN
562	539	9	4.2	N3–C4–N9 28, N3–C2–N7 24, N5–C6–N8 16	ρCN, defClO
555	533	45	3.3	O11–CL12–O15 35, N3–O11–CL12–O13 15	defClO
552	529	46	2.0	O11–CL12–O14 38, N3–O11–CL12–O1 16, N3–C4–N9–H21 12	defClO, NH
541	519	45	4.0	N3–O11–CL12–O14 46, O11–CL12–O13 17, N3–C4–N9–H21 15	defClO, NH
539	518	106	5.4	N3–C4–N9–H21 62, N3–O11–CL12–O13 12	NH
516	496	145	6.6	N3–C2–N7–H19 89	NH
435	417	22	6.4	N9–O10–H17 50, C4–N9–O10–H16 23	ρOH
404	388	13	4.4	O11–CL12–O14 48, N3–O11–CL12–O15 27, O11–CL12–O13 18	DefClO
399	383	10	4.8	O11–CL12–O13 32, O11–CL12–O15 30, N3–O11–CL12–O13 18	DefClO
375	360	16	3.2	N3–C2–N7 30, N3–C4–N9 28, C4–N9–O10 10, C2–N3–C4 10	CN
351	337	3	2.2	N5–C6–N8 54, N3–C2–N7 21, C4–N5–C6 17	CN
278	267	202	3.6	N5–C6–N8–H22 55, N5–C6–N8–H23 44	NH
266	256	97	10.3	C4–N9–O10–H17 52, N3–C4–N9–O10 24, N9–O10–H17 18	NHO
211	203	25	0.5	N9–O10 54, N3–C4–N9 15, C4–N9–O10 13, C2–N3–O11–CL12 12	NHO, NOCl
200	192	5	0.1	C4–N5–C6–N8 47, N9–O10 11, C4–N3–C2–N7 11, C2–N3–C4–N9 10	CN
193	185	3	0.6	N1–C2–N3–C4 29, C2–N3–C4–N9 21, C4–N3–C2–N7 21, C2–N3–C4–N5 19	CN
174	167	15	0.1	C2–N3–C4–N9 35, N3–O11 25, C4–N3–C2–N7 24	CN
161	155	11	0.2	C2–N3–O11–CL12 51, C4–N9–O10 45	NOCl
132	127	14	0.1	N3–O11 42, C2–N3–O11 30, C4–N3–C2–N7 14, C2–N3–C4–N9 13	L
118	113	0	0.8	N3–O11–CL12 51, C2–N3–O11–CL12 31, C2–N3–C4–N5 10	L
92	88	5	0.7	C2–N3–O11–CL12 40, N3–O11–CL12 20, C4–N9–O10 11	L
72	69	7	1.9	C2–N3–O11 85, C4–N9–O10 10	L
47	45	2	2.6	N7–C2–N3–O11 58, N3–C4–N9–O10 30, N3–O11–CL12 11	L
23	22	0	1.0	N3–O11–CL12–O13 35, N3–O11–CL12–O14 32, N3–O11–CL12–O15 30	Def ClO
−27	−26	5	1.4		

Abbreviations: ν – stretching; s – symmetric; as – antisymmetric, δ – in plane bending symmetric, γ – in plane bending antisymmetric, ω – out of plane bending symmetric, ρ – out of plane bending antisymmetric, Def – deformation of tetrahedral, L – lattice vibration.

Table 4
Calculated values of energy gap and other molecular parameters of MPM.

Molecular properties	Values
HOMO energy	−0.2877
LUMO energy	−0.0588
Energy gap	0.2289
Ionization potential (I)	0.2877
Electron affinity (A)	0.0588
Global hardness (η)	0.11445
Chemical potential (μ)	−0.17325
Global electrophilicity (ω)	0.1311298

3.2.4. Mulliken charges

Fig. 5 shows the Mulliken charges computed for MPM. In the melaminium ion all nitrogen atoms have negative charge. For two nitrogen atoms N(7) and N(9) of NH_2 group of melamine which are involved in hydrogen bonds, the charges are similar and equal to −0.47e and −0.48e respectively. Small value of charge −0.42e noticed for nitrogen atom N(8). Similar situation was observed in guanidine compounds [40]. The negative charges are balanced by positive charges of carbon and hydrogen atoms. Intra molecular hydrogen bonds have similar charges of 0.44e. Those atoms which are not involved in hydrogen bonds show small value of similar charges 0.35e. The calculated charges for carbon atoms

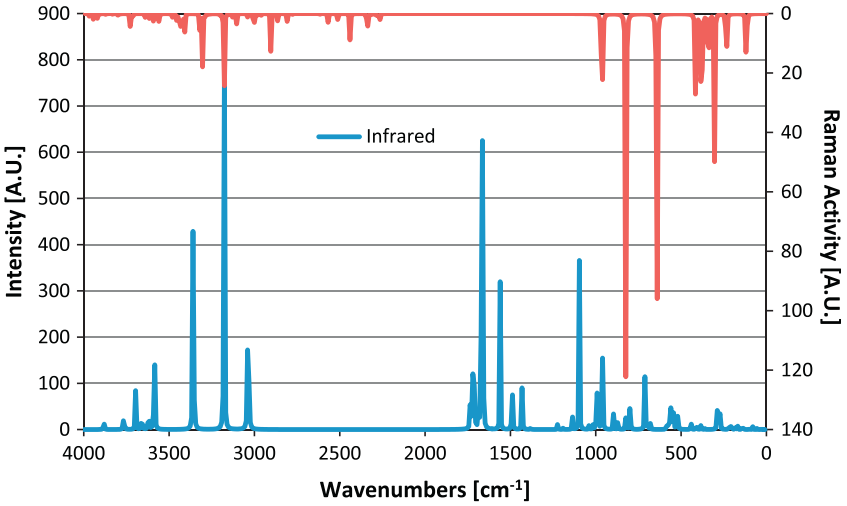

Fig. 4. Theoretical FT-IR and FT-Raman spectrum.

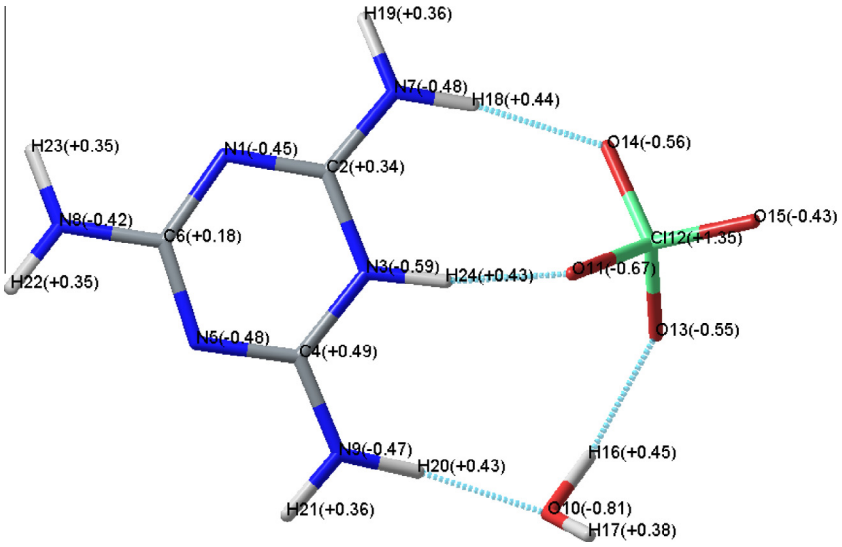

Fig. 5. Mulliken charges of MPM.

present in the melamine are positive and different. For C(6), C(2) and C(4), the calculated charges are +0.18e, +0.34e and +0.49e respectively. The charges of chlorine atom Cl(12) and oxygen atoms of perchloric acid were calculated. It was found that chlorine atoms have strong positive charge. For the oxygen atom O(14) and O(13), the calculated charges are similar (i.e.) 0.56e and 0.55e. The oxygen atom O(11) which involves in N–H···O bond has higher value of charge 0.67e.

3.2.5. HOMO–LUMO energies

The study has been extended to HOMO–LUMO analysis to calculate the energy gap. HOMO (Highest Occupied Molecular Orbitals) is an electron donor while LUMO (Lowest Unoccupied Molecular Orbital) is an electron acceptor that represents the ability to obtain an electron. The calculated HOMO–LUMO energies shows that charge transfer occurs in MPM. The atomic orbital compositions of MPM are sketched in Fig. 6. HOMO–LUMO orbital energies are given as $I = -E_{HOMO}$ and $A = -E_{LUMO}$. The energy gap between the HOMO and LUMO give the hardness and explains the charge transfer interaction that takes place within the molecule [41]. The global hardness was calculated by the expression $\eta = 1/2\ (E_{LUMO} - E_{HOMO})$. The electronic chemical potential, $\mu = 1/2\ (E_{LUMO} + E_{HOMO})$ and electrophilicity, $\omega = \mu^2/2\eta$ were also calculated and listed in Table 4.

3.3. FT-NMR analysis

The ^{1}H NMR and ^{13}C NMR spectral analysis are the important analytical techniques used to study the structure of organic compounds. The signals due to N–H and COOH protons do not show up because of fast deuterium exchange taking place in these two groups with D_2O being used as the solvent [42–44]. In the ^{1}H NMR spectrum of melamine in DMSO, all the NH_2 groups give single signal at 6.20 ppm. This peak was shifted to 7.150 ppm in the present case may be due to the addition of perchloric acid [44]. Due to hygroscopic nature of MPM crystal, strong intense water

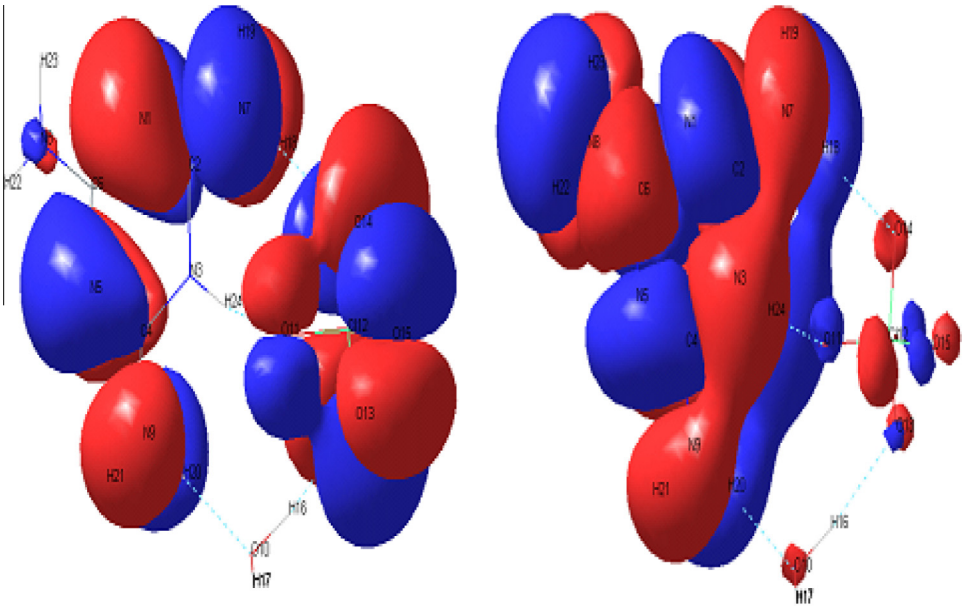

Fig. 6. Atomic orbital compositions of MPM.

signal appears at 4.695 ppm. ^{13}C NMR spectrum gives single signal at 159.68 ppm was due to 3 carbon atoms present in the triazine ring with same chemical environment. As no other peaks are observed, it is clear that the compound has been successfully synthesized and it is a pure material.

3.4. SHG test

Second harmonic generation test was performed to find the NLO property of the grown crystal by using Kurtz–Perry technique [45]. No detectable signal was observed. It is in consistency with the X-ray experiments giving centrosymmetric ($P-1$) space group of triclinic system. For centro symmetric crystals second harmonic frequency of light should not be observed [46].

4. Conclusion

Melaminium perchlorate monohydrate (MPM) single crystals have been grown by slow evaporation method. The grown crystals have been characterized by X-ray powder diffraction and it is confirmed that it crystallizes in the space group $P-1$ with triclinic geometry. The various infrared and Raman modes have been identified and assigned for MPM crystal. Several stretching and deformation modes confirm the presence of extensive intermolecular hydrogen bonding in the crystal. In general, both N–H and C–H stretching frequencies are considerably higher than either C–O or C–N stretching frequencies. Vibrational spectra have also been discussed on the basis of quantum chemical density functional theory (DFT) calculations using Firefly (PC GAMESS) version 7.1 G. The obtained theoretical vibrational frequencies are in good agreement with reported data. The Mulliken charges calculation clearly showed that for two nitrogen atoms which are involved in hydrogen bonds have similar charges and those atoms which are not involved in hydrogen bond shows smaller value of charge. Optimized geometry parameters are very well agrees with the reported one. HOMO–LUMO energies have been computed. Energy gap and other molecular properties like ionization potential, electron affinity, global hardness, chemical potential and electrophilicity were calculated. The theoretically constructed FT-IR and FT-Raman spectra of MPM coincide with the experimental one. ^{1}H NMR and ^{13}C NMR reveals the structure of MPM crystal. No detectable signal was observed during second harmonic generation.

Acknowledgements

Author (M.K.M and M.D) acknowledge Ministry of Science and Higher Education (Grant No.: NN507221840). The calculation was performed, partially on the computers of Wrocław Supercomputer and Networking Center. One of the authors (N.K. is highly thankful to Col. Vel. R. Rangarajan, Chairman, Vel Group of Institutions, Avadi, Chennai 600 062 for giving constant encouragement and kind attention towards the research work.

Appendix A. Supplementary material

Supplementary data associated with this article can be found, in the online version, at http://dx.doi.org/10.1016/j.saa.2013.04.001.

References

[1] J. Zieba-Palus, J. Mol. Struct. 327 (1999) 511–512.
[2] R.J. Meier, A. Tiller, S.A.M. Vanhommerig, J. Phys. Chem. 99 (1995) 5457–5464.
[3] W.J. Jones, W.J. Orville-Thomas, Trans. Faraday Soc. 55 (1959) 193–202.
[4] P.J. Larkin, M.P. Makowski, L.A. Food, N.B. Colthoup, Vib. Spectrosc. 17 (1998) 53–72.
[5] R.J. Meier, J.R. Maple, M.J. Hwang, A.T. Hagler, J. Phys. Chem. 99 (1995) 5445–5446.
[6] J.R. Schneider, B. Schrader, J. Mol. Struct. 29 (1975) 1–14.
[7] P.J. Larkin, M.P. Makowski, N.B. Colthoup, Spectrochim. Acta A55 (1999) 1011–1020.
[8] M.M. Zhao, P.P. Shi, Acta Cryst. E66 (2010) o1463–o1471.
[9] M.K. Marchewka, A. Pietraszko, J. Phys. Chem. Solids 64 (2003) 2169–2181.
[10] M.K. Marchewka, Mater. Lett. 58 (2004) 843–848.
[11] S. Debrus, M.K. Marchewka, M. Drozd, H. Ratajczak, Opt. Mater. 29 (2007) 1058–1062.
[12] M.K. Marchewka, Mater. Sci. Eng. B95 (2002) 214–221.
[13] M.K. Marchewka, J. Baran, A. Pietraszko, A. Haznar, S. Debrus, H. Ratajczak, Solid State Sci. 5 (2003) 509–518.
[14] M.K. Marchewka, J. Janczak, S. Debrus, J. Barana, H. Ratajczak, Solid State Sci. 5 (2003) 643–652.
[15] M. Stammler, R. Bruenner, W. Schmidt, D. Orcutt, Adv. X-Ray Anal. 9 (1966) 170–189.
[16] M. Mylrajan, T.K.K. Srinivasan, J. Raman Spectrosc. 22 (1991) 53–55.
[17] P. Czarnecki, W. Nawrocik, Z. Pajak, J. Wasicki, Phys. Rev. B49 (1994) 1511–1512.
[18] M.K. Marchewka, Bull. Korean Chem. Soc. 25 (2004) 466–470.
[19] M. Mohamed Ali Jinnah, V. Sasirekha, V. Ramakrishnan, Spectrochim. Acta A 62 (2005) 840–844.
[20] Beulah J.M. Rajkumar, V. Ramakrishnan, Spectrochim. Acta A 58 (2002) 1923–1934.
[21] S. Pandiarajan, M. Umadevi, R.K. Rajaram, V. Ramakrishnan, Spectrochim. Acta A 62 (2005) 630–636.
[22] M. Briget Mary, M. Umadevi, S. Pandiarajan, V. Ramakrishnan, Spectrochim. Acta A 60 (2004) 2643–2651.
[23] A.S. Granovsky, Firefly Version 7.1.G, <http://www.classic.chem.msu.su/gran/firefly/index.html>.
[24] RWTH Aachen, Lehrstuhl fuer Betribssysteme, 2005.
[25] G. Schaftenaar, J.H. Noordik, J. Comput. Aided Mol. Des. 14 (2000) 123–134.
[26] L. Piela, Ideas of Quantum Chemistry, Elsevier, 2007.
[27] M.K. Marchewka, M. Drozd, Spectrochim. Acta A99 (2012) 223–233.
[28] G. Fogarasi, P. Pulay, in: J.R. During (Ed.), Vibrational Spectra and Structure, vol. 13, Elsevier, New York, 1985.
[29] Y. Podolyan. <http://ccmsi.us/mask>.
[30] M.P. Fernandez-Liencres, A. Navarro, J.J. Lopez-Gonzalez, M. Fernandez-Gomez, J. Tomkinson, G.J. Kearley, Chem. Phys. 266 (2001) 1–17.
[31] M.K. Marchewka, Acta Chim. Solv. 50 (2003) 239–250.
[32] M. Drozd, M.K. Marchewka, J. Mol. Struct. THEOCHEM 716 (2005) 175–192.
[33] M.K. Marchewka, M. Drozd, A. Pietraszko, Mater. Sci. Eng. B100 (2003) 225–233.
[34] Y.L. Wang, A.M. Mebel, C.J. Wu, Y.T. Chen, C.E. Lin, J.C. Jiang, J. Chem. Soc. Farday Trans. 93 (1997) 3445–3451.
[35] S. Aruna, A. Anuradha, C. Preema Thomas, M. Gulam Mohammed, S.A. Rajasekar, M. Vimalan, G. Mani, P. Sagayaraj, Indian J. Pure Appl. Phys. 45 (2007) 524–528.
[36] B.L. Hathaway, A.E. Underhill, J. Chem. Soc. 592 (1961) 3091–3096.
[37] H. Siebert, Z. Anorg, Allg. Chem. 275 (1954) 225–240.
[38] F.A. Miller, C.H. Wilkins, Anal. Chem. 24 (1952) 1253–1294.
[39] A.M. Petrosyan, Vib. Spectrosc. 41 (2006) 97–100.
[40] Marke Drozd, Damian Dudzic, Spectrochim. Acta A 89 (2012) 243–251.
[41] R.G. Pearson, J. Am. Chem. Soc. 107 (1985) 6801–6806.
[42] S. Dhanuskodi, K. Vasantha, Cryst. Res. Technol. 39 (2004) 259–265.
[43] P.Y. Bruice, Organic Chemistry, Pearson Education (Singapore) Pvt. Ltd., 2002.
[44] Luis M. Pedroso, M. Margarida, C.A. Castro, Pedro Simoes, Antonio Portugal, Polymer 46 (2005) 1766–1774.
[45] S.K. Kurtz, T.T. Perry, J. Appl. Phys. 39 (1968) 3798–3813.
[46] V.G. Dmitriev, G.G. Gurzadyan, D.N. Nikogosyan (Eds.), Handbook of Non Linear Optical Crystals, second ed., Springer, 1997.